Journal of Constructional Steel Research 211 (2023) 108131

Contents lists available at ScienceDirect

Journal of Constructional Steel Research

journal homepage: www.elsevier.com/locate/jcsr

Design optimization of welded steel plate girders configured as a hybrid structure

Iván Negrin [a,*], Moacir Kripka [b], Víctor Yepes [a]

[a] Institute of Concrete Science and Technology (ICITECH), Universitat Politècnica de València, 46022 Valencia, Spain
[b] Graduate Program in Civil and Environmental Engineering, University of Passo Fundo, Km 292, BR 285, Passo Fundo 99052-900, RS, Brazil

ARTICLE INFO

Keywords:
Hybrid steel girder
Structural optimization
Hybrid ratio
Biogeography-based optimization

ABSTRACT

This paper implements structural design optimization to improve the economic indexes of welded steel plate girders. The optimization problem is formulated in a way that allows the use of hybrid configurations, i.e., different types of steel in the flanges and web. Besides the cross-sectional dimensions, eleven steel grades are included as optimization variables. In addition to weight and material cost, the manufacturing cost is formulated as an optimization objective, which includes seven other activities, such as welding or painting. The geometrically double symmetric I-girder design subjected to a uniform transverse load is carried out through the Eurocode 3 rules. Nine case studies are implemented by varying the girder span and load values. The results show significant differences depending on the optimization objective, especially between weight and cost optimization. On the other hand, optimization-assisted design provides solutions up to 50% more economical than traditional design methods. Hybrid-optimized configurations can also improve these indexes by about 10% compared to their homogeneous counterpart, demonstrating the applicability of this novel practice. Certain concepts highlighting mechanical properties are proposed to compare the optimal solutions for each case study. These concepts can serve as design recommendations for future projects that include this structural element. Finally, based on the research gaps and the promising results obtained, future lines of research on this topic are established.

1. Introduction

In recent decades, there has been great concern about how human activities affect our environment regarding climate change and natural resource depletion. It is due in significant part to the building sector, which is responsible for 5% of the total CO_2 emissions and one of the industries that require more materials [1]. For this reason, in 1987, the Brundtland Commission introduced the term "sustainable development" as "the development that meets the needs of the present without compromising the ability of future generations to meet their own needs" [2]. For this purpose, specific objectives have been established to improve the construction processes' sustainability, e.g., objective number 11 of the 17 sustainable development goals proposed by the United Nations: sustainable cities and communities [3].

Specific innovations in engineering structure design have been developed to achieve these objectives. Advances in manufacturing processes and material technologies have made it possible to increase the strength of available building materials. Increased strength typically means increased manufacturing costs and environmental impact, which must be considered when pursuing sustainable designs. Therefore, from a researcher's or designer's point of view, knowing how to best utilize the increased strength in structures is crucial [4]. One way to achieve this is by combining various building materials. The trend of using hybrid configurations, such as steel-concrete, concrete-high strength concrete, concrete-plastics (composites), and steel-special steels, is rising. Researchers are exploring methods to enhance the sustainability of the construction sector by leveraging the advantages of utilizing different materials (and their properties) in structural assemblies [5].

Steel I-beams are one of the most widely used elements in various types of construction worldwide. When these elements are subjected to bending, a significant portion of the stress is absorbed by the flanges, which requires them to be thicker than the web. If one wanted to increase the resistance capacity of the section by varying only the geometrical properties, the result would be a heavy and inefficient element. On the contrary, increasing the yield strength of the entire section reduces thicknesses but also increases the cost of the material. A more economically viable approach involves employing different steel types in the flanges and web, giving rise to hybrid steel elements. Many practical girders often have a smaller web area, leading to a reduced web

* Corresponding author.
E-mail address: ianegdia@doctor.upv.es (I. Negrin).

https://doi.org/10.1016/j.jcsr.2023.108131
Received 26 May 2023; Received in revised form 13 July 2023; Accepted 17 July 2023

Nomenclature

A_{fc}	effective cross area of the compression flange
$A_p(\boldsymbol{X})$	painted area per unit length
b_f	both flange width
$C_B(\boldsymbol{X})$	blasting cost
$C_C(\boldsymbol{X})$	cutting cost
C_{CBW}	cost of welding consumables
C_{CS}	cost of sawing consumables
C_{CCU}	cost of cutting consumables
$C_E(\boldsymbol{X})$	erecting cost
C_{EqE}	crane cost
C_{EnBw}	cost of welding energy
C_{EnCu}	energy consumption of the torch
C_{EnS}	cost of sawing energy
C_{LE}	erecting labor cost
$C_M(\boldsymbol{X})$	material cost
$C_P(\boldsymbol{X})$	painting cost
$C_S(\boldsymbol{X})$	sawing cost
$C_T(\boldsymbol{X})$	transportation cost
C_w	weld size factor
$C_W(\boldsymbol{X})$	welding cost
d_{ws}	distance from the workshop to the site
E	modulus of elasticity of steel
F_{sp}	parameter that depends on the plate thickness (to calculate sawing cost)
f_y	nominal yield strength of steel
f_{yf}	nominal yield strength of flanges steel
f_{yw}	nominal yield strength of web steel
h_w	web height
I_y	inertia of the cross-section with respect to the bending axis
K	coefficient to regulate the flange buckling against web
K_M	coefficient to affect the steel grade cost
K_{Mf}, K_{Mw}	coefficient to affect the steel grade cost in the flanges and web respectively
K_S	coefficient to affect the sawing cost in function of the steel grade
$K_{S,f}$, $K_{S,w}$	coefficient to affect the sawing cost in function of the steel grade in flanges and web respectively
K_W	coefficient to affect the welding cost in function of the steel grade
L	overall length of the girder
L_{Cu}	length of plate cut
L_S	distance from the lifting area to the final position of the girder
L_w	welded length
M_{cr}	critical bending moment calculated with the gross cross-section properties
M_{Ed}	maximum acting bending moment
$M_{Rk}(\boldsymbol{X})$	bending resistance of the section
$M(\boldsymbol{X})$	material cost of the girder
n_b	number of bolts per joint
p_{SB}	price of the saw blade
q	uniform load applied to the girder
q_{SLS}	serviceability limit state load
q_T	total uniform load acting on the girder
R_h	hybrid ratio
S	feeding speed of the saw
t	thickness of the plates
t_f	flanges thickness
t_w	web thickness
T_E	time to erect the girder
T_{NBW}	non-productive welding time
T_{NCu}	non-productive cutting time
T_{NS}	non-productive sawing time
$T_{PBW}(\boldsymbol{X})$	productive welding time
$T_{PCu}(\boldsymbol{X})$	productive cutting time
T_{PS}	productive sawing time
$\overline{u}$	maximum allowed displacement
u_E	utilization ratio for the erecting cost
$u_{max}(\boldsymbol{X})$	maximum displacement of the girder
$V_{c,Rd}(\boldsymbol{X})$	plastic shear resistance of the girder
V_{Ed}	maximum acting shear force
$V(\boldsymbol{X})$	volume of the girder
W_{eff}	effective modulus of the girder section
$W(\boldsymbol{X})$	weight of the girder
ΔW	term used in the formula for calculating the bending resistance according to the approximate procedure
ε	term used to classify a section
ρ	steel density
ρ_G	geometric flange-to-web ratio
ρ_{MI}	mechanical inertia flange-to-web ratio
λ_{LT}	slenderness parameter of a section
η	parameter for regulating the shear resistance

contribution. Therefore, it is also possible to achieve cost efficiency by employing lower-strength (less expensive) steel in the web compared to the flanges. The hybrid ratio (R_h) in steel girders is related to the relationship between the yield strength of the flanges and the web (f_{yf}/f_{yw}). When R_h differs from 1, the girder is classified as a hybrid element, whereas a homogeneous girder has a value of $R_h = 1$ [6]. In Veljkovic and Johansson (2004) [7], it is stated that: "An old rule of thumb says that a girder should have about the same amount of steel in the web as in the flanges together. This rule gives a reasonably optimal girder if the depth is not restricted. The web contributes 20-25% to the bending resistance for such a girder". The compilation study by Terreros-Bedoya et al. (2023) [5] concluded that the interval $1.3 \leq R_h \leq 1.6$ is where the best performance of hybrid steel beams is obtained.

Although this field needs further exploration, the initial research began in the mid-20th century. One of the early studies in this area was conducted by Frost and Schilling (1964) [8], focusing on the behavior of hybrid beams under static loading. Subsequently, Schilling (1967) [9] investigated the behavior of the web of such elements under point loads. In the same year, Fielding and Toprac [10] conducted fatigue tests on hybrid elements with A514 steel in the flanges and A36 steel in the web. One year later, Schilling [11] developed theoretical relationships for moment-curvature and moment-stress to describe the flexural behavior of composite hybrid beams. By that time, Carskaddan [12] researched the buckling resistance of the web of hybrid beams to determine the maximum slenderness ratio to prevent buckling caused by the combination of bending and shear. By that time, the use of these configurations and their benefits began to be highlighted. Therefore, the theoretical basis for considering them as a valid practice in the design of steel structures begins to be established.

More recently, practical research have been developed to study certain phenomena of this type of element in depth. In 1994, Suzuki et al. [13] studied the behavior of hybrid beams concerning local buckling. Years later, Azizinamini et al. (2007) [14] investigated the failure mechanisms of eight hybrid plate girders and compared the results with the 2003 version of the AASHTO LRFD Bridge Design Specifications. Due to the results presented in this publication, specific considerations were updated in the 2004 version of the AASHTO code. Shokouhian and Shi (2015) [15] presented a method to determine the flexural resistant capacity of homogeneous and hybrid beams regardless of the section classification. In the study, combinations are made with

Q345 and Q460 steels to achieve the different hybrid configurations. The results obtained showed close agreement with the Eurocode 3 specifications. In their research, Wang et al. (2016) [16] studied hybrid beams' flexural behavior and ductility by combining 485 W steels in the flanges with Q235 and Q345 in the web. It was concluded that using the exact geometrical dimensions, the ductility of the element decreases with increasing flange strength. Therefore, a more restrictive slenderness limit is necessary for high-strength steel structural designs. In their study, Zhu et al. (2023) [17] analyzed the flexural behavior and design of hybrid girders compared with the requirements of Eurocode 3. The results showed very interesting conclusions about the slenderness limits proposed in the Eurocode 3 standard for the classification of cross-sections. Other interesting research on hybrid elements with some innovations, such as using corrugated webs [18] or closely spaced web openings [19], has also brought diversity to the current knowledge on these elements.

However, aspects still need to be clarified, even with a certain degree of information on the subject. They still need to be explicitly reflected in the design standards for steel structures. For this reason, authors have proposed methodologies based on information from standards and some practical research. Veljkovic and Johansson (2004) [7] stated that the required standards are somewhat limited in scope and are mainly concerned with clarifying what flange or web strength value should be used in the regular design formulas. Eurocode 3 for plated structures mentions hybrid beams and states the limitation that the ratio between the elastic limits of the flanges and web should not exceed two. No further design details are given. Thus, it is suggested that the widespread use of hybrid beams would require their inclusion in codes or manuals. That is why the authors summarize the most important aspects dealt with in the Eurocode and provide additional information for dealing with the design of this type of element. Years later, Mela and Heinisuo (2014) [4] also posited that Eurocodes have virtually no rules for hybrid cross-sections. However, based on a series of experiments, the authors conclude that the existing design rules of Eurocode 3 can be used for hybrid girders with minor modifications. For example, the cross-section classification is performed using the yield strength of the compression flange, and partial web plastification is considered when assessing flexural strength. This paper also proposes an efficient methodology for the design of these elements. Instead, Wollmann (2004) [20,21] published a procedure for designing hybrid elements based on AASHTO LRFD specifications. In other standards, such as AISC 360–16, even though the yield strength between flanges and the web is differentiated, there needs to be precise information on how to proceed to design a hybrid section [5].

On the other hand, when implementing hybrid configurations, finding the optimal design is complex due to the numerous possibilities for varying cross-section dimensions and steel grades of the plates. A very efficient alternative is to use mathematical optimization theory to search for the most efficient solutions based on a given objective. Therefore, the design procedure can be formulated as an optimization problem so that the design rules of the applicable codes are met in the form of constraints. Several works have been developed in this field. Abuyounes and Adeli (1986) [22] presented an effective practical procedure to obtain the minimum weight of stiffened and unstiffened steel plate girders subjected to arbitrary loads using the General Geometric Programming (GGP) technique. The design constraints were based on the American Institute of Steel Construction (AISC) 1980 version. In the same year, Adeli and Phan [23] published an algorithm for the interactive computer-aided design of hybrid plate girders. Abuyounes and Adeli (1987) [24] repeated an experiment similar to their earlier work. Later, Dhillon and Kuo (1991) [25] presented a similar study, using the 1983 AASHTO considerations this time. Hendawi and Frangopol (1994) [26] incorporated the concept of reliability-based design into the previously stated optimization problem (which is formulated with a deterministic approach). In the same year, they also published a study adding the effects of corrosion to the problem. In their study, Mela and Heinisuo (2014) [4] used Particle Swarm Optimization to decrease the weight and the manufacturing cost of several beams by varying their span and the loading condition. Although the publications above have explored interesting variables, they have not posed problems or challenges that would allow a comprehensive exploration of the hybridization phenomenon. However, these works' results highlight the effectiveness of using hybrid configurations to reduce the weight and costs of these elements.

Therefore, it can be concluded that although the optimal design of hybrid steel I-beams has been studied to some extent, further research is still needed. It has already been shown that the lack of clarity in the standards can be made up for with methodologies based on practical studies. However, although these methodologies exist, no in-depth studies have been carried out on the feasibility of combining several types of steel in the same element. That is why this study is intended to address this issue with an approach that allows the exploration of a wide range of possible hybrid combinations. For this purpose, in addition to the geometrical variables, two other variables regulating eleven types of steel grades for the flanges and web are included. Three objective functions (weight, material cost, and manufacturing cost) are formulated to study the differences in optimizing each separately. It is important to point out that several studies have established that economic optimization is directly related to environmental benefits [27,28]. Therefore, this study serves as an essential starting point for the sustainable design of these elements. The constraints are based on the Eurocode 3 specifications, with some modifications proposed by several authors. The study highpoints the benefits of optimization-based design processes and their superiority over traditional procedures. In addition, it is highlighted that the use of hybrid configurations is a valid alternative to improve the sustainability of this type of element.

The paper is organized as follows. Section 2 explains the methodology, including the description of the case studies, the mathematical formulation of the optimization problem, and the method for solving it. It also introduces specific practical terms for analyzing the various optimal solutions. Section 3 discusses the results obtained and includes comments on future lines of research. Finally, Section 4 draws the fundamental conclusions of this study.

2. Methodology

The proposed methodology initiates by providing an overview of the case studies. Following that, the optimization problem is formulated, defining variables, objective functions, and design constraints. The subsequent section outlines the approach employed to solve this problem. Lastly, practical concepts are introduced to aid in interpreting and comparing solutions and offer design recommendations for similar elements.

2.1. Case studies description

In this research, a simply supported welded steel girder of length L subjected to a distributed load q is considered, as shown in Fig. 1. Note how the supports are shown as fork-type in the figure to emphasize that the beam model does not allow the section of the supports to rotate around the longitudinal axis. Not to be confused with the rotation produced by the bending moment caused by the distributed load, which is allowed in the simply supported condition (i.e., the bending moment at the ends is zero). The different case studies are obtained by varying the two parameters. Three values of L (6, 10, and 15 m) and q (20, 40, and 60 kN/m) are established. The full-factorial combination of these two parameters results in nine cases. A distributed load is applied since the girder is assumed to be a joist supporting a concrete slab or a similar structure. Note that even in this condition of supporting a slab (or similar structure), it is not considered that the girder is provided with sufficient transverse support to ignore the lateral-torsional buckling. It may be the case for an element forming a section of a structure with low horizontal stiffness (e.g., a bridge). That is why in the present study,

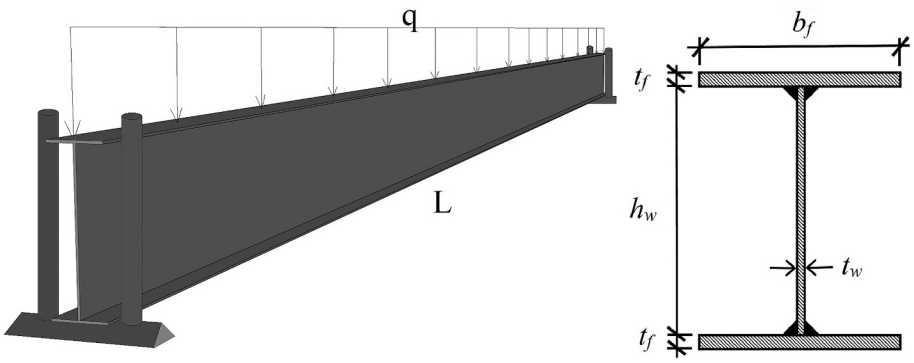

Fig. 1. Left: 3D basic case study. Right: cross-section with geometric variables.

unlike Mela and Heinisuo (2014) [4], the reduction of the bending resistance caused by lateral-torsional buckling is considered. The q load values are apparently high since it is considered the design load in the ultimate limit state, i.e., the load values coming from the upper slab have already been increased. Note that these load values are faithful to reality and could be perfectly found in a similar element of an actual structure. The self-weight of the element is also considered in the analysis.

2.2. Formulation of the optimization problem

As mentioned, the problem is formulated to optimize the girder design shown in Fig. 1 using three different objectives. The variables are formulated so that the element can have hybrid configurations (different yield strengths in the flanges and web) with the only condition that the yield strength of the flanges f_{yf} cannot exceed twice that of the web f_{yw} [29]. This formulation is based on the one made by Mela and Heinisuo (2014) [4].

2.2.1. Variables

The problem is formulated with six discrete variables. Four variables correspond to the cross-section geometry (see Fig. 1). The other two variables define the flanges and web steel grade. The vector of variables $\boldsymbol{X}$ is expressed as in Eq. (1).

$$\boldsymbol{X} = \{h_w\ t_w\ b_f\ t_f\ f_{yw}\ f_{yf}\}\ (mm) \tag{1}$$

A vector B is created to obtain the width of the plates (h_w, b_f). It consists of values ranging from 100 to 1000 mm in 10 mm intervals (100:10:1000), which makes 91 possible dimensions. In the case of the thickness (t_w, t_f), the vector T consists of 19 values, as shown in Eq. (2). The specific values assigned to the design variables accurately represent the real design scenario, where the selection of plate dimensions is limited by the availability of suitable sizes and considerations related to manufacturability [4].

$$T = \{5, 6, 8, 10, 12, 14, 15, 16, 18, 20, 22, 25, 30, 35, 40, 50, 60, 80, 100\}\ (mm) \tag{2}$$

Eleven types of steel are available for material configuration, as shown in Eq. (3).

$$M = \{S235, S275, S355, S420, S450, S500, S550, S600, S700, S890, S960\}\ (mm) \tag{3}$$

It is important to note that this study ignores the availability of the material. That is, an ideal situation is assumed where it is possible to implement any configuration. It may not be real, but it opens a broader range of possibilities to understand the phenomenon of hybrid configurations of these elements. It is worked with the nominal value of f_y of each steel grade, making the corresponding reduction according to the thickness of the plate by Table 3.1 of EN 1993-1-1 [30]. A similar reduction is assumed for the other steels that do not appear in this table.

2.2.2. Objective functions

The first and simplest objective function is the element weight, obtained by multiplying the volume of steel by its density (ρ), as shown in Eq. (4). Here, the value of ρ is assumed to be $7.85{\cdot}10^{-6}$ kg/mm^3, and L is the girder span in mm. It should be noted that all length-related parameters should be expressed in mm.

$$W(\boldsymbol{X}) = \rho L\left(2b_f t_f + h_w t_w\right)\ (kg) \tag{4}$$

The second objective function pertains to the material cost, which solely considers the cost of the element based on its volume and the type of steel used. Table 1 displays the parameters associated with the cost of each steel. For this particular function, only the value of K_M is utilized. K_M is a coefficient representing the costs of different steel types relative to a basic one. It is important to note that the price of a specific steel type can vary significantly. Thus, a 0.7 €/kg basic cost is assumed for S355 steel. The K_M coefficient expresses the remaining values relative to this basic cost. For example, S420 steel costs 1.07 as much as S355 steel. These values are obtained from [4], where cost penalties corresponding to each steel grade are equally incorporated. These values have been stated in collaboration with experts in the steel manufacturing industry. In the case of steels not covered in the abovementioned study, a linear interpolation method is employed to calculate their coefficients. Similarly, the other coefficients listed in Table 1 are also determined through linear interpolation.

Therefore, the second objective function (material cost) is reflected in Eq. (5). Here, the K_M values are divided into flanges (K_{Mf}) and web (K_{Mw}) due to the possibility of hybrid configurations.

$$M(\boldsymbol{X}) = 0.7\rho L\left(K_{Mf} 2b_f t_f + K_{Mw} h_w t_w\right)\ (€) \tag{5}$$

The third and most encompassing objective function is the manufacturing cost. In this case, erecting (C_E), painting (C_P), welding (C_W), blasting (C_B), cutting (C_C), sawing (C_S), and transportation (C_T) costs are considered in addition to the material. Therefore, the function is reflected in Eq. (6).

Table 1
Cost parameters according to steel grades.

Steel grade	K_M	C_w	Welding (K_W)	Sawing (K_s)
S235	0.88	0.34	0.79	0.88
S275	0.92	0.41	0.86	0.92
S355	1.00	0.55	1.00	1.00
S420	1.07	0.66	1.11	1.07
S450	1.10	0.71	1.16	1.10
S500	1.15	0.80	1.25	1.15
S550	1.19	0.80	1.31	1.19
S600	1.23	0.81	1.38	1.23
S700	1.30	0.82	1.50	1.30
S890	1.44	0.84	1.74	1.44
S960	1.50	0.84	1.83	1.50

$$C_M(\boldsymbol{X}) = M(\boldsymbol{X}) + C_E(\boldsymbol{X}) + C_P(\boldsymbol{X}) + C_W(\boldsymbol{X}) + C_B(\boldsymbol{X}) + C_C(\boldsymbol{X}) + C_S(\boldsymbol{X}) + C_T(\boldsymbol{X})\ (€) \tag{6}$$

The erecting cost is obtained as in Eq. (7).

$$C_E(\boldsymbol{X}) = T_E \frac{C_{LE} + C_{EqE}}{u_E}\ (€) \tag{7}$$

Where C_{LE} is the labor cost (3.10 €/min), C_{EqE} is the crane cost (1.35 €/min), and the utilization is $u_E = 0.36$. The time to erect the girder is obtained as in Eq. (8). Here, L_S is the distance from the lifting area to the final position (15,000 mm) and n_b is the number of bolts per joint (6 in this case). It should be noted that the erection cost only depends on the length of the girder since the number of bolts per joint and the crane's capacity are fixed.

$$T_E(\boldsymbol{X}) = \frac{L}{30\,000} + \frac{L_S}{27\,000} + 2(0.5n_b - 0.42) + \frac{L_S}{36\,000}\ (min) \tag{8}$$

The alkyd painting system of Haapio (2012) [31] is assumed in this study. For its calculation, the expression shown in Eq. (9) is used.

$$C_P(\boldsymbol{X}) = 4.17 \bullet 10^{-6} L A_P(\boldsymbol{X}) + 0.36 L b_f \bullet 1 \bullet 10^{-6}\ (€) \tag{9}$$

Here, $A_P(\boldsymbol{X}) = 3b_f + 4t_f + 2h_w - 2t_w$ (mm^2/mm) is the painted area per unit length. It should be noted that drying is included in the painting cost calculation, which is reflected in the second term of the equation. It is also assumed that it is unnecessary to paint the top surface of the upper flange due to the upper structure (e.g., a concrete slab).

Assuming an automatic submerged arc welding process, the cost of welding the plates to form the girder is expressed as in Eq. (10).

$$C_W(\boldsymbol{X}) = 2K_W[1.36(T_{NBW} + T_{PBW}(\boldsymbol{X})) + T_{PBW}(\boldsymbol{X})(C_{CBW} + C_{EnBW})]\ (€) \tag{10}$$

Where C_{CBW} and C_{EnBW} are 1.36 and 0.08 €/min respectively. Also, $T_{NBW} = 6.25$ min. The productive time is obtained as in Eq. (11).

$$T_{PBW}(\boldsymbol{X}) = \frac{7.85 \bullet 10^{-6} L_w a_w^2}{14} = \frac{7.85 \bullet 10^{-6} L_w C_w^2 t_w^2}{14}\ (min) \tag{11}$$

Here, L_w (mm) is the welded length (L), and C_w is the weld thickness factor that depends on the steel grade of the web (see Table 1). To define the C_w factor, the total resistance property of the weld is assumed. For example, for S355, the weld thickness is $a_w = 0.55t_w$ and so on. These values of C_w are obtained from [32,33], according to [4]. The base expression of $C_w(\boldsymbol{X})$ refers to welding a flange with the web, so, it is multiplied by 2 to obtain the total value of the productive time to weld the two flanges. In order to take into account the increased cost of welding high-strength steels, factors K_W are introduced (see Table 1). They are used by multiplying the costs of Eq. 10 by the factor corresponding to the maximum grades of the plates to be welded.

It is assumed that the blasting and cutting costs do not depend on the quality of the steel. The shot blasting cost depends on the number of plates and the length of each plate to be blasted before welding. For the girder, the plate lengths are L (mm). Thus, the blasting cost is obtained as in Eq. (12).

$$C_B(\boldsymbol{X}) = 3 \bullet 3.64 \bullet 10^{-4} L\ (€) \tag{12}$$

Additionally, the cutting cost can be expressed as in Eq. (13).

$$C_C(\boldsymbol{X}) = 1.32(T_{NCu} + T_{PCu}(\mathbf{X})) + T_{PCu}(\mathbf{X})(C_{CCu}(\mathbf{X}) + C_{EnCu})\ (€) \tag{13}$$

Here, the non-productive time $T_{NCu} = 3.0$ min. Depending on the plate thickness, flame or plasma cutting is used. For plate thicknesses up to 30 mm, plasma cutting is used, where the productive time is:

$$T_{PCu}(\boldsymbol{X}) = \frac{L_{Cu}(\boldsymbol{X})}{8.92t^2 - 486.87t + 8115.8}\ (min) \tag{14}$$

were t (mm) is the plate thickness. The cost of cutting consumables is $C_{CCu} = 0.38$ €/min. The cost of energy is $C_{EnCu} = 0.12$ €/min. The length of the cut L_{Cu} is $2(b_f + L)$ for the flanges and $2(h_w + L)$ for the web, in mm.

Otherwise, for flame cutting productive time and consumable costs are expressed as in Eqs. (15) and (16) respectively.

$$T_{PCu}(\boldsymbol{X}) = \frac{L_{Cu}(\boldsymbol{X})}{-4.19t + 658.67}\ (min) \tag{15}$$

$$C_{CCu}(\boldsymbol{X}) = 0.22 + 4.18\left(1 \bullet 10^{-5} t^2 + 0.001t + 0.0224\right)\ (€/min) \tag{16}$$

The energy consumption of the torch is neglected ($C_{EnCu} = 0$). Overall, to obtain the cutting cost, Eq. (13) must be used for the web and both flanges separately. Thus, the cutting of the flange plates is obtained by multiplying Eq. (13) by 2.

The sawing cost is calculated according to Eq. (17).

$$C_S(\boldsymbol{X}) = 1.20(T_{NS} + 2T_{PS}(\mathbf{X})) + 2T_{PS}(\mathbf{X})(C_{CS}(\mathbf{X}) + C_{EnS})\ (€) \tag{17}$$

The non-productive time $T_{NS} = 4.5 + L/20000$ min. The cost of energy $C_{EnS} = 0.02$ €/min. The productive time T_{PS} depends on the position of the cross section when it is sawn. It is assumed that the girder is laid on its side such that the flanges are considered to be sawn vertically and the web horizontally. For assessing the higher steel grades, cost factors are introduced to the production time (see Table 1), as can be checked in Eq. (18).

$$T_{PS}(\boldsymbol{X}) = K_{S,f} \frac{b_f}{0.9St_f} + K_{S,w} \frac{h_w t_w}{8800}\ (min) \tag{18}$$

Here, S is the feeding speed of the saw. It depends on the plate thickness as defined in Table 2. The terms $K_{S,f}$ and $K_{S,w}$ represents the values of K_S of Table 1, and are in function of the steel grades of the flanges and web, respectively. The consumables cost C_{CS} includes the wear of the saw blades. It can be obtained through Eq. (19).

$$C_{CS}(\boldsymbol{X}) = p_{SB} \frac{2(b_f t_f) + (h_w t_w)}{11.88 \bullet 10^6 F_{sp}(t_f) T_{PS}(\boldsymbol{X})}\ (€/min) \tag{19}$$

Here F_{sp} is a parameter that depends on the plate thickness as display in Table 2, and p_{SB} is the price of the saw blade (100 €). The terms defining the geometrical properties of the section (b_f, t_f, h_w, t_w) can be seen in Fig. 1.

Finally, the transportation cost is defined as follows.

$$C_T(\boldsymbol{X}) = \begin{cases} V(\boldsymbol{X})(0.0106 d_{ws} + 1.2729), if \dfrac{W(\boldsymbol{X})}{V(\boldsymbol{X})} \le 264 \\ W(\boldsymbol{X})\left(4 \bullet 10^{-5} d_{ws} + 4.8 \bullet 10^{-3}\right), otherwise \end{cases}\ (€) \tag{20}$$

According to the conditional definition, the transportation cost is calculated based on the volume of the beam if the weight to volume ratio $\boldsymbol{W(X)/V(X)}$ falls below the specified limit. If the ratio exceeds the limit, the cost is instead determined by the weight of the beam. The volume occupied by the beam is $V(\boldsymbol{X}) = Lb_f(2t_f + h_w) \bullet 1 \bullet 10^{-9}$ (m^3). $\boldsymbol{W(X)}$ should be expressed in kg. The distance from the workshop to the site d_{ws} is assumed to be 200 km.

2.2.3. Constraints

The constraints of a design optimization problem ensure that this design is correct. These constraints are based on Eurocode 3 [29,30]. In

Table 2
Saw feeding rate S and parameter F_{sp} according to Mela and Heinisuo (2014) [4].

Plate thickness (mm)	S (mm/min)	F_{sp}
5	120	0.40
6–10	100	0.45
11–15	90	0.50
16–20	80	0.55
21–25	70	0.60
26–30	60	0.65
31–35	40	0.70
≥ 36	50	0.80

this case, the resistance to bending, shear, and three types of buckling (lateral-torsional, shear, and flange buckling against the web) are checked. The deflection of the beam at the center of its span in the serviceability limit state is also checked. This methodology is based on those proposed by Veljkovic and Johansson (2004) [7] and Mela and Heinisuo (2014) [4]. In this case, the bending-shear interaction is discarded because the element is simply supported, so this phenomenon does not significantly affect the girder. When the bending is maximum, the shear is zero, and vice versa. For space reasons, not all the corresponding equations are shown. In any case, the reader may refer to the references.

2.2.3.1. Bending resistance. The bending resistance constraint is shown in Eq. (21). Here, $M_{Rk}(\boldsymbol{X})$ is the bending resistance of the section and M_{Ed} is the maximum bending moment, obtained in the center of the girder span as $q_T L^2/8$. The sub-index T of the distributed load refers to the consideration of the self-weight in addition to the load q (q + self-weight).

$$M_{Rk}(\boldsymbol{X}) \geq M_{Ed} \tag{21}$$

As mentioned, the calculation of the bending resistance is based on the proposal of Mela and Heinisuo (2014) [4]. Considering that the methodology proposed here is cumbersome when the top flange or web belongs to a class higher than 2, an approach proposed by Veljkovic and Johansson (2004) [7] is used. Since the section type will influence the bending resistance, the first step is to proceed to its classification. It is done according to Table 5.2 of EN 1993–1–1 [30]. The web is classified as a part subject to bending, and the top flange is a compression part. The bending resistance of the cross-section is obtained as the sum of the bending resistances of its parts. In classes 1 and 2, plastic design is applied, and M_{Rk} is the plastic moment of the cross-section as computed in Eq. (22).

$$M_{Rk}(\boldsymbol{X}) = f_{yf}\left(b_f t_f\right)\left(h_w + t_f\right) + \left(f_{yw}(h_w t_w)h_w\right)/4 \tag{22}$$

However, if any of the elements of the section are in a class higher than 2, the simplified procedure is used. First, the flanges are assumed to be in class 3 or lower. The effective cross-section of the web should be calculated using the yield strength of the compression flange. The resulting effective cross-section is usually not symmetric, and the resistance calculation is iterative (Mela and Heinisuo, 2014) [4]. Nevertheless, Eq. (23) is an approximate formula for the calculation of the bending strength of an I-girder with equal flanges published by Höglund (1973) [34] and adjusted by Veljkovic and Johansson (2001) [35] to comply with Eurocode 3–1-5 resistance.

$$M_{Rk}(\boldsymbol{X}) = f_{yf}\left(W_{eff} - \Delta W\right) \tag{23}$$

It is from this basic formula that two procedures are differentiated. If the web is in class 3, it is considered the effective modulus of the section W_{eff} calculated following the principles shown in Fig. 2 according to Eurocode 3–1-1 [30] and Veljkovic and Johansson (2004) [7], and ΔW is obtained according to Eq. (25). If the web is in class 4, Eq. (24) is used.

$$W_{eff} = W\left[1 - 0.1\frac{h_w t_w}{b_f t_f}\left(1 - 124\varepsilon\frac{t_w}{h_w}\right)\right] \; when \; \frac{h_w}{t_w} \geq 124\varepsilon \tag{24}$$

$$\Delta W = h_w^2 t_w \left(1 - \frac{f_{yw}}{f_{yf}}\right)^2 \left(2 + \frac{f_{yw}}{f_{yf}}\right) \Big/ 12 \tag{25}$$

$$\varepsilon = \sqrt{235/f_{yf}} \tag{26}$$

According to Eurocode 3–1-5, the elastic modulus of section W must be calculated at the mid-plane of the flanges.

2.2.3.2. Lateral-torsional buckling. The reduction factor for lateral-torsional buckling can be the same as for homogeneous beams. It should be applied to the bending resistance of the cross-section calculated according to the rules mentioned above. The reduction procedure can be found in Eurocode 3–1-1 ([30], Section 6.3.2). The slenderness parameter (λ_{LT}) can be calculated from Eq. (27), where M_{cr} is the critical bending moment according to elastic stability theory calculated with the gross cross-section properties.

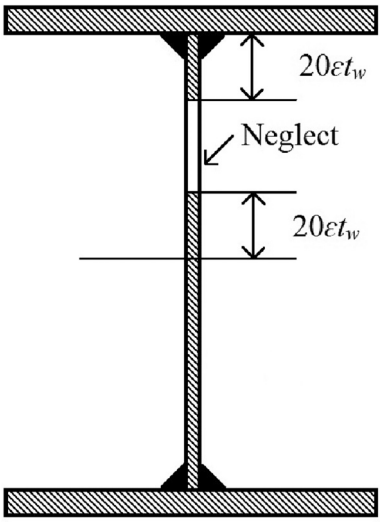

Fig. 2. Effective cross sections with class 3 webs and class 1 or 2 flanges according to Eurocode 3–1-1.

$$\lambda_{LT}(\boldsymbol{X}) = \sqrt{M_{Rk}(\boldsymbol{X})/M_{cr}} \tag{27}$$

2.2.3.3. Shear resistance and buckling. The shear resistance constraint is shown in the Eq. (28). Here, $V_{Ed} = q_T L/2$ and $V_{c,Rd}(\boldsymbol{X})$ is the plastic shear resistance, obtained according to ([29], Section 5). In the expression of plastic shear strength, the shear area contains the parameter η which depends on the web steel grade. According to ([30], Clause 5.1(2)), $\eta = 1.20$ if $f_{yw} \leq 460$ N/mm^2 and $\eta = 1.00$ otherwise.

$$V_{c,Rd}(\boldsymbol{X}) \geq V_{Ed} \tag{28}$$

In the case of shear buckling, according to ([30], Clause 5.1(2)) this phenomenon must be considered if $h_w/t_w > 72\varepsilon/\eta$. Then, the element shall be provided with transverse stiffeners in the supports according to ([30], Clause 5.1(2)) and ([30], Section 9.3).

2.2.3.4. Flange buckling against the web. To avoid the possibility of buckling of the compression flange in the web plane, the ratio h_w/t_w must meet the criterion established in Eq. (29) ([30], Clause 8(1)).

$$\frac{h_w}{t_w} \leq k\frac{E}{f_{yf}}\sqrt{\frac{h_w t_w}{A_{fc}}} \tag{29}$$

Here, E is the modulus of elasticity of steel (210,000 MPa), A_{fc} is the effective cross area of the compression flange, and $k = 0.40$ if plastic moment resistance is used. Otherwise, if elastic moment resistance is employed, $k = 0.55$.

2.2.3.5. Girder deflection. One of the most critical constraints for this type of element (and even more so with hybrid configurations) is the one related to the stiffness. Since the maximum displacement (u_{max}) occurs at the center of the span, the constraint is written as in Eq. (30).

$$u_{max}(\boldsymbol{X}) \leq \overline{u} \tag{30}$$

Here, $\overline{u}$ is the maximum allowed displacement. For this study, a commonly used value such as L/400 is implemented. The maximum displacement is obtained from Eq. (31). Here, q_{SLS} is the serviceability

limit state load (in N/mm), considered $0.75q$, and I_y is the inertia of the cross-section with respect to the bending axis (in mm^4).

$$u_{max}(\boldsymbol{X}) = \frac{5}{384}\frac{q_{SLS}L^4}{EI_y(\boldsymbol{X})} \tag{31}$$

2.2.4. Mathematical formulation

In summary, the problem is formulated as shown in Eq. (32). Here, $f(\boldsymbol{X})$ can be one of the three defined functions: the weight $W(\boldsymbol{X})$, the material cost $M(\boldsymbol{X})$, and the manufacturing cost $C_M(\boldsymbol{X})$.

$$\begin{aligned}
&minf(\boldsymbol{X})\\
&\text{Such that } M_{Ed} \le M_{Rk}(\boldsymbol{X})\\
&V_{Ed} \le V_{c,Rd}(\boldsymbol{X})\\
&\frac{h_w}{t_w} \le k\frac{E}{f_{yf}}\sqrt{\frac{h_w t_w}{A_{fc}}}\\
&u_{max}(\boldsymbol{X}) \le \overline{u}\\
&f_{yf} \le 2f_{yw}\\
&b_f, h_w \in B\\
&t_f, t_w \in T\\
&f_{yf}, f_{yw} \in M
\end{aligned} \tag{32}$$

It is important to note that the problem has six discrete variables and comprises a space of 3.62×10^8 possible solutions. It is not a large-scale problem, but as stated by Mela and Henisiuo (2014) [4], it is a nonlinear optimization problem. There are certain discontinuities in the constraint functions, for example, in the bending resistance constraint function in regions where the cross-section class changes. Thus, the mathematical properties of the constraints make finding the global optimum tricky. It makes most of the classical nonlinear discrete optimization methods inapplicable. Instead, population-based heuristics are an excellent alternative to deal with this type of problem.

2.3. Solution to the optimization problem

To solve the problem posed in Eq. (32), it was decided to use a relatively new heuristic called Biogeography-Based Optimization (BBO), proposed by Simon (2008) [36]. This heuristic has proven to be very efficient in discrete structural design optimization problems. In Negrin et al. (2021) [37], it was successfully applied to optimize the reinforced concrete frame structure design. In this research, a deep analysis of its behavior in this problem was made through an extensive parameter tuning process. In Negrin and Chagoyén (2022) [28] it was also used in a similar study, achieving equally satisfactory results. It is important to note that the method's parameters were tuned to solve the problem L = 15 m and q = 60 kN/m for each of the three objectives. This added to the experience gained in previous work, makes each problem solved in the most efficient way possible. Heuristic optimization guarantees valid designs that comply with the constraints imposed on the problem and provide outstanding quality solutions regarding the optimization objective. In this research, efforts have been made to ensure that the final result is the global optimum, either by tuning the method's parameters to maximize its performance or by performing several optimization processes (with the corresponding statistical verification) to ensure that the solution offered is the global optimum.

Negrin et al. (2021) [37] discuss why this methodology performs so well in discrete optimization. It lies in the recombination and mutation operator used. Classical evolutionary algorithms (EAs), such as genetic algorithms (GA), combine complete candidate solutions. That is, two solutions ("parents" in the GA terminology) are selected and combined to obtain the new solution ("child"). It means that the procedure is performed from solution to solution. In the case of BBO, this process of combining solutions is performed at the level of the variables ("genes" in the GA terminology or "species" in the BBO one). Thus, new solutions are formed by combining variables from several previous candidate solutions. Therefore, while classical EAs, such as GAs, perform the analysis using entire prior individuals, BBO performs this analysis on a variable-by-variable basis. When the GA combines two solutions to create a new one, BBO can obtain solutions from more than two previous candidates. In addition, the combination and mutation operators can affect the variable involved in the same process of getting new solutions. That is, the mutation is performed at the variable level and not at the level of the entire solution. Therefore, a solution can be affected several times by the mutation. Refer to the references cited above for detailed information on how the algorithm works.

2.4. Some terms for interpreting solutions

One of the important aspects of structural design optimization is how to interpret the results. Simply providing the optimal values of the variables may not be meaningful. On the contrary, if specific terms are established that help to extrapolate the results to other instances, the phenomenon can be better understood. These terms can also be used as design recommendations for other research or real-life challenging problems.

In addition to presenting the optimal values of each variable for each case study, representative graphical solutions (scaled cross-sections) are shown. It helps to visualize the solutions' geometrical differences depending on the problem type. However, this concept is not helpful as a design recommendation. Instead, a measure can be established that relates the difference between the steel area of the flanges and the web. It is similar to the "steel ratio" concept used in reinforced concrete to establish the difference between the steel area and that of the cross-section concrete. In this case, the implemented term is the "geometric flange-to-web ratio" (ρ_G) and is calculated as shown in Eq. (33) (for a geometrically double symmetric I-girder).

$$\rho_G = \frac{2{*}b_f t_f}{h_w t_w} \tag{33}$$

Nevertheless, this concept loses relevance when it comes to a hybrid configuration, where the steel grade used in the different components is also significant in addition to the geometry. An already introduced term that conceptualizes this phenomenon is the hybrid ratio (R_h), calculated according to Eq. (34).

$$R_h = \frac{f_{yf}}{f_{yw}} \tag{34}$$

But as with ρ_G, the hybrid ratio alone does not explain the overall mechanical phenomenon. The geometric concepts established so far are directly related to the area. However, a better measure of the distribution of a surface is the inertia, which includes the area and its position concerning the centroid of the figure. That is why another term called "mechanical inertia flange-to-web ratio" (ρ_{MI}) is established. It is obtained as in Eq. (35).

$$\rho_{MI} = \frac{f_{yf}}{f_{yw}}\frac{I_{yf}}{I_{yw}} \tag{35}$$

Here, I_{yf} and I_{yw} are the inertia of the two flanges and the web with respect to respect to the bending axis, respectively.

3. Results and discussion

The results and their discussion are focused on three fundamental aspects. First, the influence of the optimization target is addressed. For

Table 3
Results when optimizing using each of the three proposed objectives and their influence on the others for L = 6 m and the three loading conditions.

Opt. target	Flanges		Web		W (kg)	Mat. cost (€)	Man. cost (€)
	bf x tf (mm)	Steel	hw x tw (mm)	Steel			
q = 20 kN/m							
Weight	100 × 5	S 700	400 × 5	S 550	1607	130	398
Mat. cost	140 × 5	S 500	400 × 5	S 275	1736	114	292
Man. cost	120 × 6	S 450	430 × 5	S 235	1810	115	285
q = 40 kN/m							
Weight	100 × 5	S 960	580 × 5	S 890	1971	185	490
Mat. cost	240 × 6	S 450	430 × 5	S 235	2634	167	348
Man. cost	240 × 6	S 450	430 × 5	S 235	2634	167	348
q = 60 kN/m							
Weight	120 × 5	S 960	610 × 5	S 890	2326	224	533
Mat. cost	170 × 5	S 960	660 × 5	S 600	2644	218	505
Man. cost	300 × 6	S 450	510 × 6	S 235	3537	219	418

Table 4
Results when optimizing using each of the three proposed objectives and their influence on the others for L = 10 m and the three loading conditions.

Opt. target	Flanges		Web		W (kg)	Mat. cost (€)	Man. cost (€)
	bf x tf (mm)	Steel	hw x tw (mm)	Steel			
q = 20 kN/m							
Weight	100 × 5	S 960	800 × 5	S 890	4124	403	769
Mat. cost	170 × 5	S 890	730 × 5	S 450	4488	355	660
Man. cost	320 × 5	S 550	620 × 5	S 275	5450	366	627
q = 40 kN/m							
Weight	100 × 10	S 960	920 × 5	S 890	5349	529	912
Mat. cost	250 × 5	S 960	890 × 5	S 600	6021	506	874
Man. cost	410 × 5	S 700	780 × 5	S 355	7130	508	820
q = 60 kN/m							
Weight	100 × 15	S 960	980 × 5	S 960	6367	651	1055
Mat. cost	500 × 5	S 700	970 × 5	S 355	9060	624	970
Man. cost	500 × 5	S 700	970 × 5	S 355	9060	624	970

Table 5
Results when optimizing using each of the three proposed objectives and their influence on the others for L = 15 m and the three loading conditions.

Opt. target	Flanges		Web		W (kg)	Mat. cost (€)	Man. cost (€)
	bf x tf (mm)	Steel	hw x tw (mm)	Steel			
q = 20 kN/m							
Weight	110 × 16	S 890	1000 × 5	S 700	10,160	1054	1542
Mat. cost	490 × 5	S 550	960 × 5	S 275	12,633	845	1264
Man. cost	170 × 12	S 700	990 × 5	S 355	10,929	846	1229
q = 40 kN/m							
Weight	160 × 25	S 700*	1000 × 6	S 700	16,638	1426	1967
Mat. cost	860 × 5	S 600	1000 × 5	S 450	18,334	1325	1900
Man. cost	570 × 8	S 600	1000 × 5	S 355	18,042	1337	1808
q = 60 kN/m							
Weight	550 × 12	S 600*	1000 × 6	S 600	23,842	1947	2542
Mat. cost	670 × 10	S 600	1000 × 6	S 450	24,443	1902	2473
Man. cost	580 × 12	S 600	1000 × 6	S 355	24,766	1906	2409

* Solutions with higher quality steels are not possible as in similar cases (Tables 3 and 4) since the buckling constraint of the compression flange is not met (see Eq. (29)).

this purpose, the results are compared when optimizing using (1) weight, (2) material cost, and (3) manufacturing cost. The second point, and the main contribution of this research, is focused on the advantages of applying design optimization and using hybrid configurations over traditional homogeneous ones. Thirdly, analyzing the optimal solutions allows for providing specific design recommendations based on the terms introduced in Section 2.4. Finally, based on the results and the gaps found in this topic, several comments on future lines of research are provided.

3.1. Targeting influence

One of the primary interrogations of this research is what results are obtained depending on the optimization objective. Tables 3, 4, and 5 show significant differences in the optimal solutions, especially between the lightest and the most economical girders.

In the first case of Table 3 (L = 6 m, q = 20 kN/m), obtaining the lightest beam means increasing the material cost by 14% and the manufacturing cost by 40%. Getting the beam with the lowest material cost increases the weight by 8% and the manufacturing cost by 2%. In obtaining the most economical beam, the weight increases by 13% and the material cost by <1%. For the second case (q = 40 kN/m), the lighter beam increases the material cost by 11% and the manufacturing cost by 29%. Note that the best solution for the two cost objectives is the same. Thus, the cheaper beam means a 34% heavier element. In the third case (q = 60 kN/m), the lighter beam is 3% and 28% more expensive

considering only the material and the overall cost, respectively. The cheaper element considering only the material cost is 14% heavier and 21% more expensive in general. The optimal configuration in total cost terms is 52% heavier and the difference with the material cost best solution is minimal. For this element, using the weight as a target decreases the differences as the load increases. On the contrary, using the total cost results in heavier elements when the element is more stressed. The differences when using both costs are generally low, becoming negligible when using the total cost.

On the other hand, Table 4 shows the results related to the 10 m girder. For the first case (q = 20 kN/m), the lighter element is 14% more expensive allowing for only the material and 23% more expensive in view of the overall cost. Considering only the material, the less expensive beam is 9% heavier and 5% more expensive considering the other activities. Regarding the overall cost, the cheapest beam is 32% heavier, and the difference with the material cost is 3%. For the second case (q = 40kN/m), the lighter beam increases the material cost by 5% and the total cost by 11%. The beam that is cheaper to build is 33% heavier, and the difference with the material cost is negligible. Optimizing the weight for the third load condition (q = 60 kN/m) increases the material cost by 4% and the total cost by 9%. The solution by optimizing both costs is the same, 42% heavier than the solution obtained by optimizing the weight. It is curious to note the difference in optimizing costs with weight, even though the differences are not so significant when optimizing weight. This phenomenon is explained in the section comparing the different optimal solutions. For this element (L = 10 m), like the previous one (L = 6 m), as the load increases, using weight as the objective function offers cheaper solutions.

Finally, optimizing the weight of the third girder (15 m, Table 5) for the first loading condition increases the material cost by 25%, as well as the manufacturing cost. Optimizing the material cost increases the element weight by 24% and the total cost by 3%. Optimizing the latter increases the weight by a surprising 8%, and the increase in material cost is minimal. For the second loading condition, the lighter beam is obtained by increasing the material and manufacturing costs by 8% and 9%, respectively. Optimizing the material cost increases the material cost by 10% and the total cost by 5%. Optimizing the manufacturing cost leads to another surprising 8% increase in weight and a 1% increase in material cost. Finally, for the last loading condition, the results are pretty homogeneous. Optimizing the weight increases the material and manufacturing costs by only 2 and 6%, respectively. Optimizing the material cost increases the weight by 3%, as well as the manufacturing cost. Optimizing the latter increases the weight by only 4%, and the increase in material cost is negligible. In this case, it is surprising that manufacturing cost optimization tends to offer lighter solutions than material cost optimization. On the other hand, it can be seen that the differences are smaller than for the other girders.

As can be seen, there are marked differences when optimizing weight and both types of costs. These differences are reduced as the girder span and load are increased. It is due to the possibility of varying the costs depending on the material, i.e., these objectives perceive the type of steel grade, while the weight does not since all steels are assumed to have the same density. Therefore, the lightest element is not the most economical, and vice versa. The optimization of both costs does provide very similar results. Fig. 3 shows how the manufacturing cost behaves when optimizing each objective. Each curve is the average performance of 10 optimization processes. Both costs behave similarly while optimizing weight gives lower quality results (regarding manufacturing cost).

One aspect of the optimization highlighted in this figure is that the weight function is the easiest to optimize, as seen in its more stable curves. Here it can be seen that the algorithm is able to find the global optimum (or at least one of excellent quality) much faster. On the contrary, optimizing the material cost seems the most difficult, sometimes needing more iterations than the rest to reach a good solution.

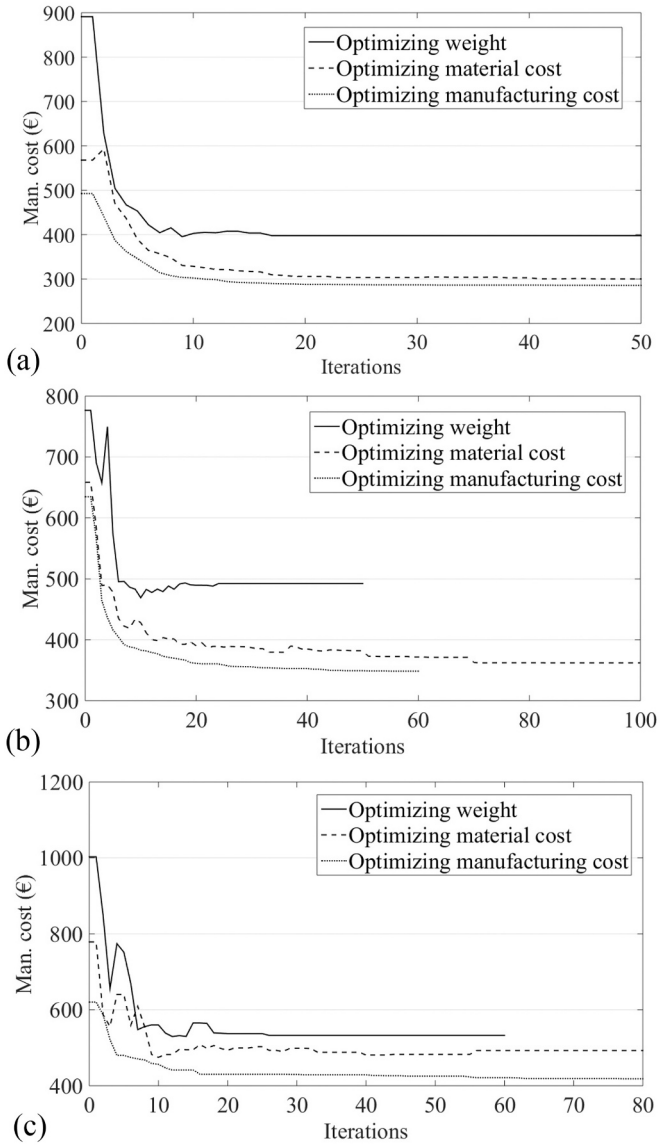

Fig. 3. Behavior of the manufacturing cost when optimizing the 6 m beam for the three proposed objectives, (a) q = 20 kN/m, (b) q = 40 kN/m, and (c) q = 60 kN/m.

3.2. Benefits of design optimization and hybridization

As mentioned, the principal value of this research is to highlight the importance of design optimization with the addition of hybrid configurations. Table 6 shows the optimal results of three types of design. The first has a traditional approach. Using a finite element software (SAP2000), the lightest profile that meets the design constraints is selected from a catalog of profiles. The software itself does this. However, it does not identify the violation of the stiffness constraint. Thus, it is necessary to manually check this condition and look for alternatives through an iterative process. Once the section is defined, it is checked using the programmed routine for the girder calculation, and the costs are obtained. The second design method is aided by the optimization process but without the possibility of using hybrid configurations, i.e., $f_{yf} = f_{yw}$. It demonstrates the benefit of hybridization by comparing homogeneous and hybrid optimized solutions. The third design method is optimization with the formulation that allows the hybrid configuration.

Fig. 4 is the comparison expressed in percent of the results shown in Table 6. As can be seen, the differences in manufacturing cost between

Table 6
Results from applying three different types of design using manufacturing cost as the objective.

Des. method	Flanges		Web		Man. cost (€)
	bf x tf (mm)	Steel	hw x tw (mm)	Steel	
			L = 6 m		
q = 20 kN/m					
Traditional	200 × 14	S 355	220 × 8	S 355	515
Opt. homog.	210 × 5	S 275	400 × 5	S 275	308
Opt. hybrid	120 × 6	S 450	430 × 5	S 235	285
q = 40 kN/m					
Traditional	200 × 14	S 355	310 × 10	S 355	626
Opt. homog.	120 × 10	S 275	900 × 5	S 275	417
Opt. hybrid	240 × 6	S 450	430 × 5	S 235	348
q = 60 kN/m					
Traditional	180 × 18	S 355	380 × 12	S 355	788
Opt. homog.	140 × 10	S 355	950 × 5	S 355	483
Opt. hybrid	300 × 6	S 450	510 × 6	S 235	418
			L = 10 m		
q = 20 kN/m					
Traditional	260 × 18	S 355	380 × 10	S 355	1135
Opt. homog.	130 × 10	S 355	940 × 5	S 355	691
Opt. hybrid	320 × 5	S 550	620 × 5	S 355	627
q = 40 kN/m					
Traditional	250 × 20	S 355	650 × 12	S 355	1499
Opt. homog.	140 × 10	S 700	940 × 5	S 700	907
Opt. hybrid	410 × 5	S 700	780 × 5	S 355	820
q = 60 kN/m					
Traditional	270 × 22	S 355	720 × 14	S 355	1836
Opt. homog.	170 × 10	S 890	970 × 5	S 890	1051
Opt. hybrid	500 × 5	S 700	970 × 5	S 355	970
			L = 15 m		
q = 20 kN/m					
Traditional	330 × 22	S 355	580 × 14	S 355	2585
Opt. homog.	190 × 10	S 600	1000 × 5	S 600	1346
Opt. hybrid	170 × 12	S 700	990 × 5	S 355	1229
q = 40 kN/m					
Traditional	360 × 30	S 355	650 × 18	S 355	3729
Opt. homog.	540 × 8	S 600	1000 × 5	S 600	1917
Opt. hybrid	570 × 8	S 600	1000 × 5	S 355	1808
q = 60 kN/m					
Traditional	450 × 22	S 355	930 × 18	S 355	4046
Opt. homog.	550 × 12	S 600	1000 × 6	S 600	2541
Opt. hybrid	580 × 12	S 600	1000 × 6	S 355	2409

the solutions optimized with hybrid configurations and those obtained with a traditional design range from 40 to 52%, demonstrating the advantage of optimizing the design of structures. The graph shows the most significant differences are for the highest load, except for the 15 m girder. It is due to the constraint of $h_w \leq 1000$ mm (upper bound). When this parameter is limited in a very stressed element, it is impossible to find an optimal configuration as it was being done for the other cases. Note that the other two load cases tend to increase the difference for larger spans. On the other hand, the graph on the right shows the advantage of using hybrid configurations over their homogeneous counterparts. It is curious that contrary to what was believed, hybridization provides improvements of up to 17% for small spans, although, for the lowest load case, the difference decreases. Either way, it can be seen that using different types of steel in the flanges and the web is a beneficial practice.

Fig. 5 shows a breakdown of the main elements involved in calculating manufacturing cost and their potential influence on the differences above. Regarding optimizing the design, the leading cause of the significant cost reduction lies in the material. The optimization algorithm aims to find a configuration where the cross-sectional area is better distributed, resulting in a reduction in material quantity. Additionally, while the algorithm seeks solutions requiring less material, it also significantly reduces welding costs, as observed. Other noticeable differences are observed in "other" costs. Interestingly, optimized solutions generally exhibit higher consumption in the painting activity. On the other hand, in the comparison between homogeneous and hybrid optimal elements, it can be seen that, similar to traditional design solutions, material and welding costs are the most influential factors. The possibility of using different steel grades opens up a range of combinations that improve the structural efficiency of the element and seek more cost-effective mechanical configurations (geometry + material). The influence of welding costs is evident in the most stressed elements, where homogeneous solutions require a section with stronger steel. Alternatively, hybrid configurations enhance the quality of the steel only in the flanges, while the web, which is crucial for welding the element, is made of lower-grade steel.

3.3. Comparison of solutions

This section compares the solutions obtained for the different design procedures applied to the case studies. First, a scaled cross-section representation of several results is made to visualize significant differences.

Fig. 6 shows the results of the three girders under the first loading condition and the 10 m girder for all three conditions. It can be seen that the traditional design (D1) offers much more compact solutions. In contrast, weight optimization (D2) and manufacturing cost optimization with homogeneous configurations (D3) offer the most slender solutions. The main difference between D3 and the optimized solutions based on manufacturing cost with hybrid configurations (D5) is that the latter tends to use more material in the flanges, either by increasing thickness (t_f) or length (b_f) alternatively. The sections also tend to be less slender, with exceptions (L = 6 and 15 m, q = 20 kN/m). On the other hand, the difference between D5 with the elements obtained by optimizing the material cost with hybrid configurations is similar to the previous

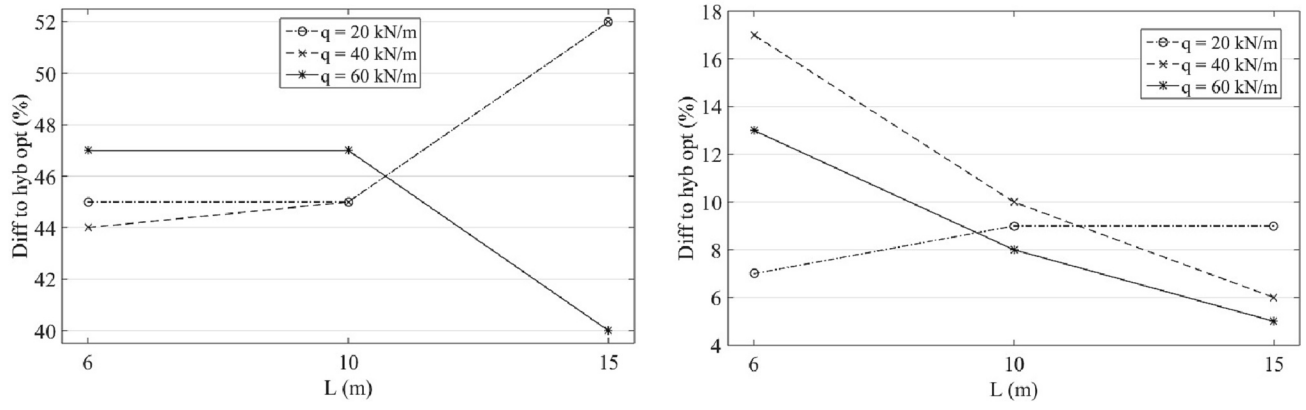

Fig. 4. Percentage differences of using the design methods in Table 6 concerning manufacturing cost optimization with hybrid configurations. Left: traditional design, right: optimization with homogeneous configurations.

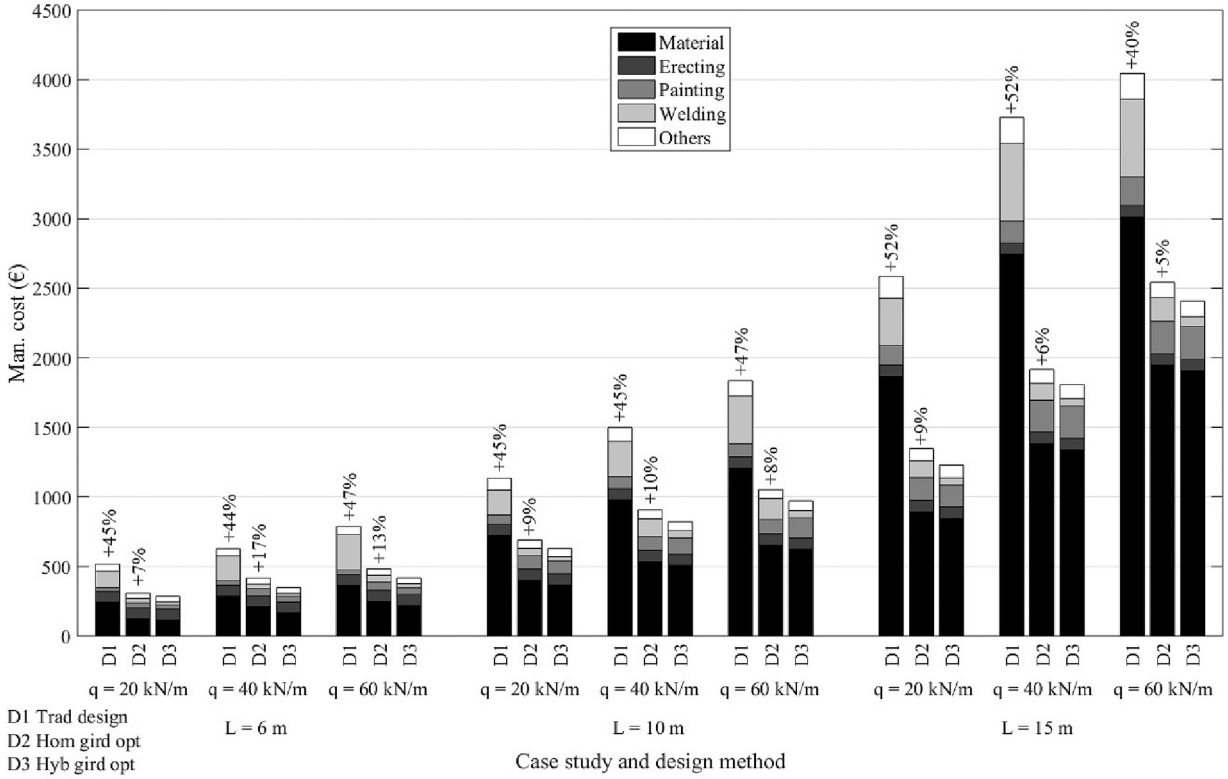

Fig. 5. Breakdown of the main elements that make up the optimal solutions for each case study using the manufacturing cost as the optimization objective.

example. However, these solutions tend to look more alike.

3.3.1. *Geometric flange-to-web ratio*

One element that provides more geometric information than the above comparison is the geometric flange-to-web ratio (ρ_G)) defined in Section 2.4 (see Eq. (33)). Fig. 7 shows these ratios for the nine case studies and the five design (D) approaches. It is essential to highpoint that these plots (also those in Fig. 8) provide specific design recommendations. Note that the most comprehensive design (D5, optimized solutions based on manufacturing cost with hybrid configurations) is emphasized, represented by the red line.

In this case, it can be seen that the traditional design tends to have configurations with more material in the flanges than the web, as opposed to the results of weight optimization. It is due to obtaining very slender elements with tiny flanges, as discussed in the previous section. The results when applying D3 and D4 are pretty similar in this term. On the other hand, it can be seen how the results of D5 are the most "stable" about the equality of material in the flanges and web. However, as in almost all solutions (except those of traditional design), there is a tendency to increase the ρ_G values for the cases of the most stressed elements. It is due, in part, to the web height restriction, which causes more material to be concentrated in the flanges to cope with the increased stresses. It is essential to highlight that there is an agreement between the results of D5 and the comment in the introduction: "An old rule of thumb says that a beam should have approximately the same amount of steel in the web as in the flanges together".

3.3.2. *Hybrid ratio*

The previous comparison is purely geometric, i.e., it does not consider the type of material used in the section. That is why another of the terms mentioned before (not only in Section 2.4) is the hybrid ratio, which helps us identify the relationship between the two steel grades used in the flanges and web.

As can be appreciated in Table 7, highlighting hybrid configurations with low R_h in weight optimization is important. It is also worth noting the use of high-quality steels to decrease the volume of the element. In the latest solutions (for the most stressed elements), the algorithm forces the search for homogeneous variants with lower-grade steels compared to other solutions due to the compression flange buckling constraint (see Eq. (29)). On the other hand, configurations with higher hybrid ratios are used in the material cost optimization. However, these ratios are lower than those obtained in manufacturing cost optimization. It can be attributed to the reduced welding costs, which, as mentioned before, are significantly reduced with hybrid configurations. It is important to emphasize hybrid designs for small spans and low load values. It is also important to note that the optimum R_h values are higher than the range recommended in the introduction (1.30–1.60). It should be noted that it is obtained from research to date in which the formulations still need to exploit the potential of hybrid configurations fully. In addition, most of the works optimized the weight of the material, which is more in agreement with the results obtained in this study.

3.3.3. *Mechanical inertia flange-to-web ratio*

Other indicator that can better express the contribution of each element to the total resistance of the section is the mechanical moment of inertia ρ_{MI}, as established in Section 2.4. Fig. 8 is similar to 7, but in function of ρ_{MI}. It can be established that the trends are similar. However, the designs that allow hybrid configurations change their position concerning the others. The introduction stated that to achieve an optimal configuration, "the web should contribute 20-25% to the bending resistance". For this experiment, the most stable values of ρ_{MI} for D5 are around 3. It means that the flanges influence the bending resistance of the section three times more than the web, contributing a quarter of the total, i.e., 25%. There is also a trend towards obtaining slightly higher values of ρ_{MI}. It means that the contribution of the web decreases, falling within the range above. In general, the term ρ_{MI} helps

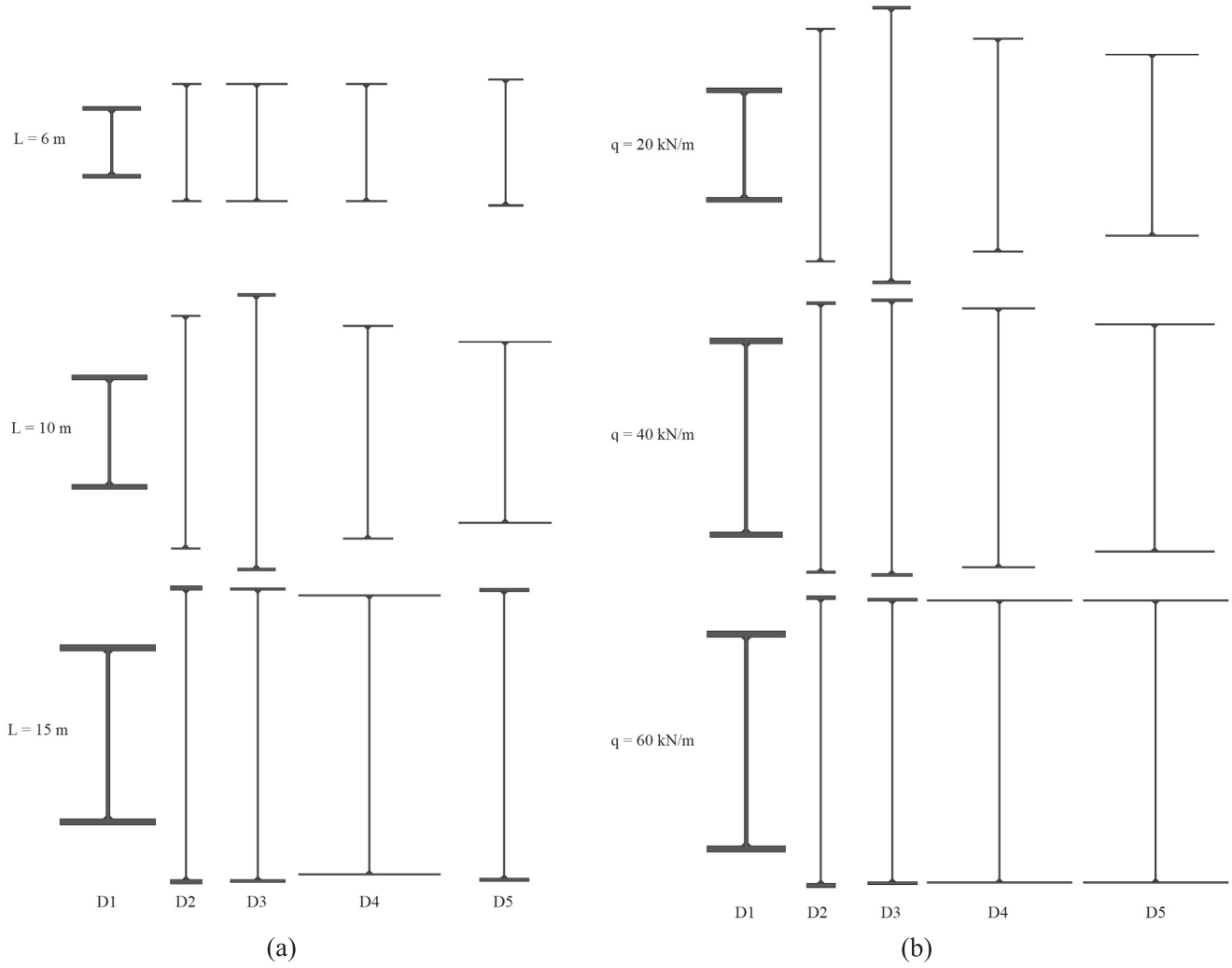

Fig. 6. Scaled cross-sections obtained by the five types of design (D). Left: the three girders for q = 20 kN/m. Right: girder of L = 10 m for the three load conditions. D1: Traditional design, D2: Weight optimization, D3: Manufacturing cost homogenous girder optimization, D4: Material cost hybrid girder optimization and D5 is the manufacturing cost hybrid girder optimization.

better understand how the flanges and web contribute to the total flexural strength of the section.

3.4. Some comments on future research

One of the research gaps in the addressed topic is the need for more clarity regarding using hybrid configurations. Even though standards such as the Eurocode or AASHTO LRFD consider different steel grades in the flanges and web, some aspects should be addressed more clearly. Therefore, the first point to be developed would be to summarize and validate the results published in this field through experimentation, to update and make the information in the standards more explicit. It is imperative, given the development of research that has demonstrated that the use of hybrid configurations can be an excellent alternative to improve the design efficiency of this type of element.

On the other hand, once the efficiency of hybridization in simple elements has been demonstrated, further exploration of their use in other typologies is needed. Reinforced steel beams optimized with hybrid configurations can be a structurally efficient element. More complex structures, such as steel box girders, can also significantly benefit from hybridization. Many types of cross-sections commonly used in bridges are based on using I-section girders, similar to those addressed in this study. Other composite typologies based on combining steel and concrete (e.g., steel-concrete composite decks) can also significantly improve their sustainability indexes through optimization and hybridization. Formulating problems that contemplate hybridization not only transversal (as in this study) but also longitudinal can be another interesting variant. This wide range of structural solutions should be optimized for design using more comprehensive approaches that include environmental, social, and durability criteria. This optimization should not only be limited to the design stage but also consider all phases of the structure's life cycle. For this purpose, implementing Life Cycle Analysis within the optimization process is essential.

One aspect of great novelty, and to some extent surprising, is the efficiency of the proposed methodology for small spans and relatively light load configurations. It opens another research branch on using these elements and their variants in buildings. It should be noted that technical standards on using structural steel in buildings such as AISC 360–16 need to include relevant information on this practice. In addition, the results show that weight and economic optimization tend to offer quite different solutions. It may be contradictory since decreasing weight can be fundamental to building design. Therefore, optimization problems of steel building structures with the possibility of hybrid configurations could be a fascinating problem to solve.

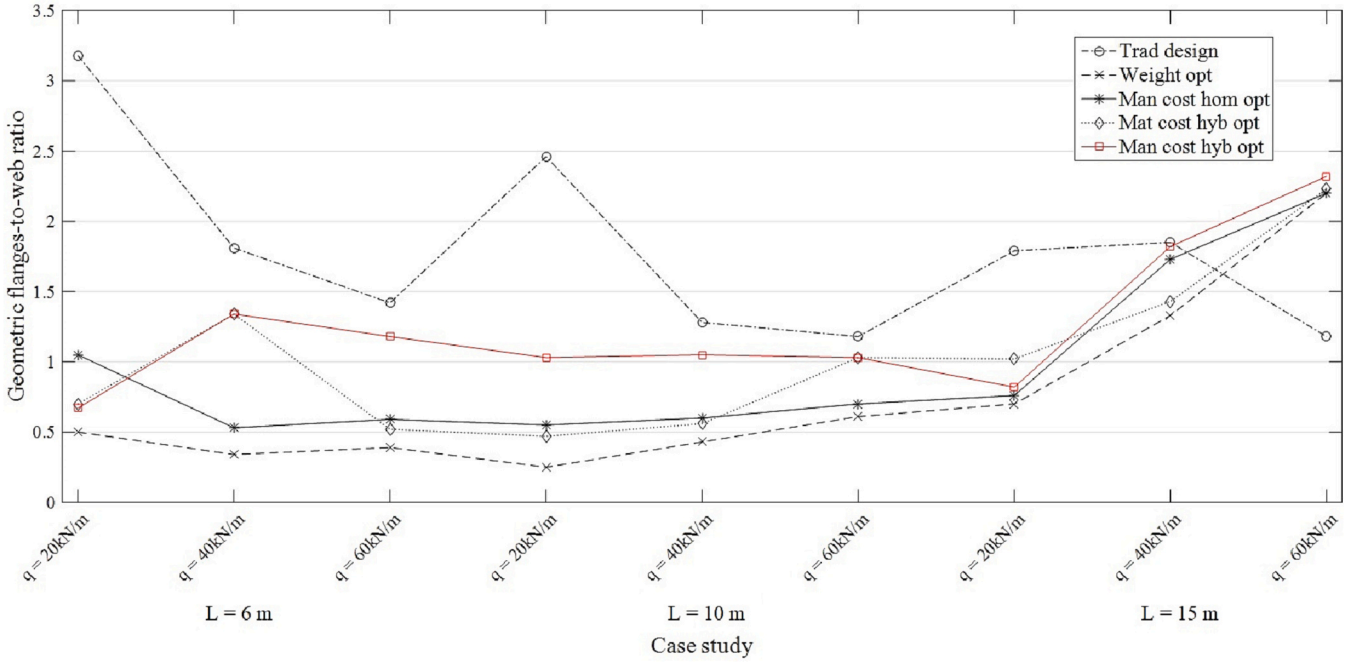

Fig. 7. Optimal geometric flanges-to-web ratios for the nine case studies using the manufacturing cost as the optimization objective.

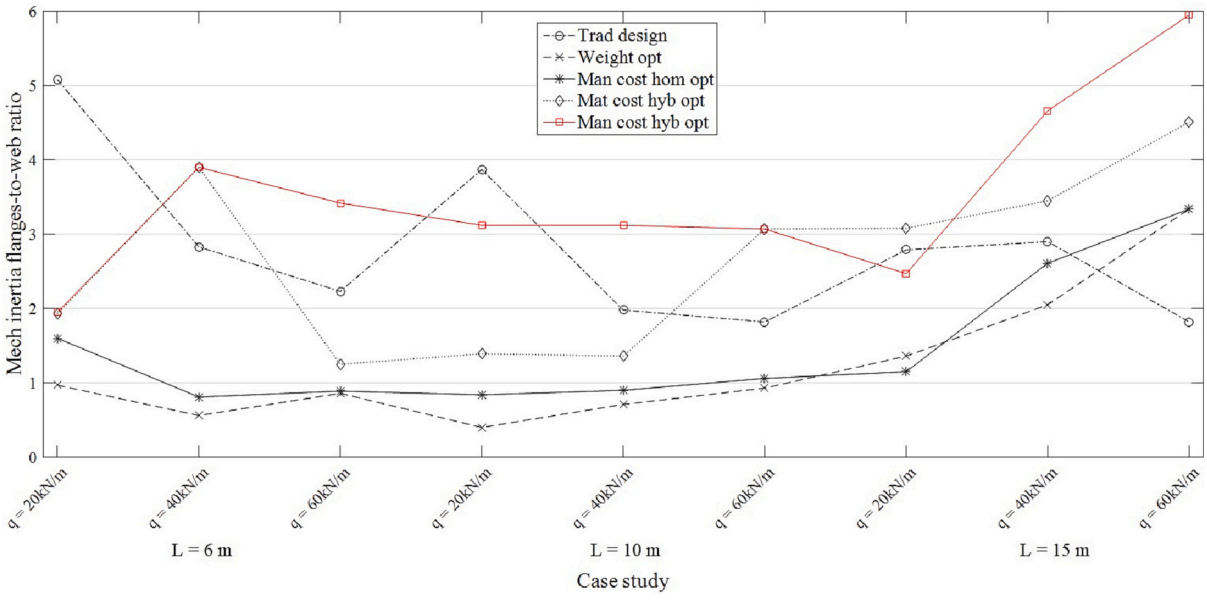

Fig. 8. Optimal flanges-to-web mechanical inertia ratios for the nine case studies using the manufacturing cost as the optimization objective.

Table 7
Hybrid ratios for the nine case studies as a function of the three proposed optimization objectives.

L (m)	q (kN/m)	Weight opt.	Mat. cost opt.	Man. cost opt.
			R_h	
6	20	1.27	1.82	1.91
	40	1.08	1.91	1.91
	60	1.08	1.60	1.91
10	20	1.08	1.98	2.00
	40	1.08	1.60	1.97
	60	1.00	1.97	1.97
15	20	1.27	2.00	1.97
	40	1.00	1.33	1.69
	60	1.00	1.33	1.69

4. Conclusions

This study explores the possibility of implementing hybrid configurations in welded steel plate girders to improve their economic indexes. For this purpose, an optimization problem is formulated, which, unlike previous studies, includes eleven different steel grades to obtain a broader range of possible hybrid solutions. Three objective functions are proposed as optimization objectives. One of these is the manufacturing cost, composed of essential elements such as material cost, but includes seven other activities such as painting or welding. The solutions obtained using this objective differ from those obtained using a common one, such as weight.

The most important conclusion of the study lies in the superiority of optimization-assisted design processes, which yield results up to 50%

more economical than traditional methods. It also highlights the effectiveness of hybrid configurations over their homogeneous counterparts. Designs can be up to 17% more economical using different types of steel in the flanges and web. The effectiveness of hybrid configurations for small-span girders is also very interesting, which opens another line for future research on using these elements in buildings. The study also provides design recommendations using several proposed terms to identify optimal solutions' geometrical and mechanical properties.

Another point to highlight is the analysis of future lines of research based on the aspects highlighted in the study. One of these points is that the current standards for steel structures need to contain sufficiently explicit rules to design these elements. The role of partial web plastification and its effect on cross-section classification and bending resistance should be addressed. Moreover, considering the good results of this study, the implementation of hybrid configurations should be extrapolated to more complex structures, such as box girders. Also, the more comprehensive optimization of these structures by performing Life Cycle Analysis is another work to be developed.

CRediT authorship contribution statement

Iván Negrin: Conceptualization, Methodology, Software, Investigation, Formal analysis, Visualization, Writing – original draft. **Moacir Kripka:** Conceptualization, Writing – review & editing, Supervision, Project administration. **Víctor Yepes:** Conceptualization, Resources, Supervision, Project administration, Writing – review & editing, Funding acquisition.

Declaration of Competing Interest

The authors declare that they have no known competing financial interests or personal relationships that could have appeared to influence the work reported in this paper.

Data availability

Data will be made available on request.

Acknowledgments

This work was supported by the grant PID2020-117056RB-I00, which was funded by MCIN/AEI/10.13039/501100011033 and by "ERDF A way of making Europe". Grant PRE2021-097197 funded by MCIN/AEI/10.13039/501100011033 and by FSE+.

References

[1] I.J. Navarro, V. Yepes, J.V. Martí, F. González-Vidosa, Life cycle impact assessment of corrosion preventive designs applied to prestressed concrete bridge decks, J. Clean. Prod. 196 (2018) 698–713, https://doi.org/10.1016/j.jclepro.2018.06.110.
[2] J.J. Pons, V. Penadés-Plà, V. Yepes, J.V. Martí, Life cycle assessment of earth-retaining walls: an environmental comparison, J. Clean. Prod. 192 (2018) 411–420, https://doi.org/10.1016/j.jclepro.2018.04.268.
[3] United Nations, Sustainable Development Goals, Sustainable Cities and Communities. https://www.un.org/sustainabledevelopment/cities/.
[4] K. Mela, M. Heinisuo, Weight and cost optimization of welded high strength steel beams, Eng. Struct. 79 (2014) 354–364, https://doi.org/10.1016/j.engstruct.2014.08.028.
[5] A. Terreros-Bedoya, I. Negrin, I. Payá-Zaforteza, V. Yepes, Hybrid steel girders: review, advantages and new horizons in research and applications, J. Constr. Steel Res. 207 (2023), 107976, https://doi.org/10.1016/j.jcsr.2023.107976.
[6] A.S. Kulkarni, L.M. Gupta, Experimental investigation on flexural response of hybrid steel plate girder, KSCE J. Civ. Eng. 22 (7) (2018) 2502–2519, https://doi.org/10.1007/s12205-017-0313-7.
[7] M. Veljkovic, B. Johansson, Design of hybrid steel girders, J. Constr. Steel Res. 60 (2004) 535–547, https://doi.org/10.1016/S0143-974X(03)00128-7.
[8] R.W. Frost, C.G. Schilling, Behavior of hybrid beams subjected to static loads, J. Struct. Div. 90 (3) (1964) 55–88, https://doi.org/10.1061/JSDEAG.0001109.
[9] C.G. Schilling, Web crippling tests on hybrid beams, J. Struct. Div. 93 (1) (1967) 59–70, https://doi.org/10.1061/JSDEAG.0001624.
[10] D.J. Fielding, A.A. Toprac, Fatigue Tests of Hybrid Plate Girders under Combined Bending and Shear [Online], Available at: http://library.ctr.utexas.edu/digitized/TexasArchive/phase1/96–2-CHR.pdf, 2023.
[11] C.G. Schilling, Bending behaviour of composite hybrid beams, J. Struct. Div. 94 (1968) 1945–1964, https://doi.org/10.1061/JSDEAG.0002038.
[12] P.S. Carskaddan, Shear buckling of unstiffened hybrid beams, J. Struct. Div. 94 (1968) 1965–1990, https://doi.org/10.1061/JSDEAG.0002039.
[13] T. Suzuki, T. Ogawa, K. Ikarashi, A study on local buckling behavior of hybrid beams, Thin-Walled Struct. 19 (1994) 337–351, https://doi.org/10.1016/0263-8231(94)90038-8.
[14] A. Azizinamini, J.B. Hash, A.J. Yakel, R. Farimani, Shear capacity of hybrid plate girders, J. Bridg. Eng. 12 (5) (2007) 535–543, https://doi.org/10.1061/(asce)1084-0702(2007)12:5(535).
[15] M. Shokouhian, Y. Shi, Flexural strength of hybrid steel I-beams based on slenderness, Eng. Struct. 93 (2015) 114–128, https://doi.org/10.1016/j.engstruct.2015.03.029.
[16] C. Wang, L. Duan, Y. Frank Chen, S. Wang, Flexural behavior and ductility of hybrid high performance steel I-girders, J. Constr. Steel Res. 125 (2016) 1–14, https://doi.org/10.1016/j.jcsr.2016.06.001.
[17] Y. Zhu, X. Yun, L. Gardner, Behaviour and design of high strength steel homogeneous and hybrid welded I-section beams, Eng. Struct. 275 (2023), 115275, https://doi.org/10.1016/j.engstruct.2022.115275.
[18] Y.B. Shao, Y.M. Zhang, M.F. Hassanein, Strength and behaviour of laterally-unrestrained S690 high-strength steel hybrid girders with corrugated webs, Thin-Walled Struct. 150 (2020), 106688, https://doi.org/10.1016/j.tws.2020.106688.
[19] R.A. Bhat, L.M. Gupta, Behaviour of hybrid steel beams with closely spaced web openings, Asian J. Civ. Eng. 22 (2021) 93–100, https://doi.org/10.1007/s42107-020-00300-9.
[20] G.P. Wollmann, Steel girder design per AASHTO LRFD specifications (part 1), J. Bridg. Eng. ASCE 9 (4) (2004).
[21] G.P. Wollmann, Steel girder design per AASHTO LRFD specifications (part 2), J. Bridg. Eng. ASCE 9 (4) (2004).
[22] S. Abuyounes, H. Adeli, Optimization of steel plate girders via general geometric programming, J. Struct. Mech. 14 (4) (1986) 501–524, https://doi.org/10.1080/03601218608907531.
[23] H. Adeli, K. Phan, Interactive computer-aided design of non-hybrid and hybrid plate girders, Comput. Struct. 2 (3) (1986) 267–289, https://doi.org/10.1016/0045-7949(86)90033-7.
[24] S. Abuyounes, H. Adeli, Optimization of hybrid steel plate girders, Comput. Struct. 27 (5) (1987) 575–582, https://doi.org/10.1016/0045-7949(87)90072-1.
[25] B.B.S. Dhillon, C. Kuo, Optimum design of composite hybrid plate girders 117 (7) (1991) 2088–2098, https://doi.org/10.1061/(ASCE)0733-9445(1991)117:7(2088).
[26] S. Hendawi, D.M. Frangopol, Design of composite hybrid plate girder bridges based on reliability and optimization, Struct. Saf. 15 (1–2) (Aug. 1994) 149–165, https://doi.org/10.1016/0167-4730(94)90057-4.
[27] V. Penadés-Plà, T. García-Segura, V. Yepes, Accelerated optimization method for low-embodied energy concrete box-girder bridge design, Eng. Struct. 179 (2019) 556–565, https://doi.org/10.1016/j.engstruct.2018.11.015.
[28] I. Negrin, E. Chagoyén, Economic and environmental design optimisation of reinforced concrete frame buildings: a comparative study, Structures 38 (2022) 64–75, https://doi.org/10.1016/j.istruc.2022.01.090.
[29] EN 1993–1–5, Eurocode 3: Design of Steel Structures. Part 1–5: Plated Structural Elements, CEN, 2006.
[30] EN 1993–1–1, Eurocode 3: Design of Steel Structures. Part 1–1: General Rules and Rules for Buildings, CEN, 2005.
[31] J. Haapio, Feature-Based Costing Method for Skeletal Steel Structures Based on the Process Approach, Ph.D. thesis., Tampere University of Technology, 2012.
[32] EN 1993–1–8, Eurocode 3: Design of Steel Structures. Part 1–8: Design of Joints, CEN, 2005.
[33] EN 1993–1–12, Eurocode 3: Design of Steel Structures. Part 1–12: Additional Rules for the Extension of EN 1993 Up to Steel Grades S700, CEN, 2007.
[34] T. Höglund, Design of Thin Plate I Girders in Shear and Bending with Special Reference to Web Buckling, Institutionen for Byggnadsstatik KTH, 1973. Bulletine no. 94.
[35] M. Veljkovic, B. Johansson, Design for buckling of plates due to direct stress, in: Nordic Steel Construction Conference, Helsingfors, 2001, pp. 729–736.
[36] D. Simon, Biogeography-based optimization, IEEE Trans. Evol. Comput. 12 (6) (2008) 702–713.
[37] I. Negrin, D. Roose, E. Chagoyén, G. Lombaert, Biogeography-based optimization of RC structures including static soilstructure, Struct. Eng. Mech. 80 (3) (2021) 285–300, https://doi.org/10.12989/sem.2021.80.3.285.